Wind load characteristics of large billboard structures with two-plate and three-plate configurations

Dahai Wang[1,2], Xinzhong Chen[*2], Jie Li[3] and Hao Cheng[1]

[1]Department of Civil Engineering, Wuhan University of Technology, Wuhan Hubei, 430070, China
[2]National Wind Institute, Department of Civil, Environmental and Construction Engineering, Texas Tech University, Lubbock TX, 79409, USA
[3]The State Key Laboratory on Disaster Reduction in Civil Engineering, Tongji University, Shanghai, 200092, China

Abstract. This paper presents a wind tunnel study of wind loads of the large billboard structures with two-plate and three-plate configurations. Synchronous dynamic pressures on the surfaces of plates are measured, and the characteristics of local pressures, integrated forces on each individual plate and on the overall structures are investigated. The influences of wind direction and plate configuration on wind load characteristics, and the contributions of overall crosswind load and torque to the stress responses are examined. The results showed that the wind load characteristics of windward plate in both two- and three-plate configurations are very similar. The contribution of overall crosswind load makes the total resultant force from both alongwind and crosswind loads less sensitive to wind direction in the case of three-plate configuration. The overall torque is lower than the value specified in current codes and standards, and its contribution is less significant in both two-plate and three-plate configurations.

Keywords: billboards; wind loading; wind tunnel tests; wind pressures; drag force; torque

1. Introduction

Large billboards are commonly used along highways for displaying signs and information. In addition to the widely used single plate configuration, the recent trend in the sign industry is to use two-plate and three-plate configurations as shown in Figs. 1(a) and 1(b). These structures are typically 20 to 50 m high above the ground and with large rectangular plates about 20 to 30 m in width and 5 to 8 m in height. The billboards are supported by enclosed truss or frames which are then supported by a mono-pole. Post-disaster investigations have reported many damages and failures of the large billboards due to typhoon or hurricanes or other types of strong winds (e.g., Tamura 2009, Song 2009, An 2009). These damages and failures can be local damage of the connection bolts between the cladding plate and supporting structure, damage of the plate skin due to the intensive local wind pressures on the plate, damage of plate supporting frame, bucking of the supporting column, and failure of its foundation bolt connection as shown in Figs. 1(c)-1(e).

To date, extensive wind tunnel studies have been conducted to investigate the drag force and

---

∗Corresponding author, Professor, E-mail: xinzhong.chen@ttu.edu

torque of a free standing wall or a single rectangular plate in boundary layer turbulent flows (e.g., Letchford 1994, 1999, 2001). The influences of aspect ratio, clearance ratio, porosity of plate and the wind direction on wind load were examined. The results of these wind tunnel studies were reflected in the design code and standards, where the drag force coefficient is directly specified and the torque is given in terms of a horizontal eccentricity (ASCE/SEI 7-10; AS/NZS 1170.0:2011). Drag forces on a rectangular louvered panel with the different porosity ratio were obtained in a wind tunnel study (Zuo *et al.* 2011). The surface pressure distributions and overall integrated forces on static and auto-rotating flat plates have been compared by wind tunnel testing (Martinez-Vazquez 2010). Meyer *et al.* (2015) carried out experimental study of wind-induced vibration of variable massage signs due to vortex shedding and galloping.

(a) Two-plates

(b) Three-plates

(c) Damage of plate cladding

(d) Failure of plate supporting structure

(e) Failure of foundation

Fig. 1 Typical descriptions and damages or failures of large billboards

In addition to a single plate and box configuration, integral wind loads on two-plate billboards and V-shaped billboards have also been investigated through wind tunnel studies and field measurements (Warnitchai 2006, Zuo *et al*. 2014, Smith *et al*. 2014), as these types of configurations are now commonly used in practice. The results showed that the drag force coefficient and eccentricity are similar to the case of a single plate configuration. Gu *et al*. (2015) discussed the characteristics of pressure distribution on the surfaces of two-plate and three-plate billboards, but the characteristics of net pressure, integrated drag forces and torques on plates were not addressed. Although extensive research efforts have been made to investigate the integrated wind loading on billboards, few studies have been conducted to examine the dynamic wind pressure distributions on billboards with two, especially three rectangular plates.

This study presents a comprehensive wind tunnel investigation on the characteristics of local net wind pressures on each plate and integrated drag forces and torques on billboards structures with two-plate and three-plate configurations are conducted. The characteristics of wind pressure distribution, the integrated drag force and torque of individual plate, and overall drag force and torque on the supporting structures are examined using the pressure measurements at different wind directions. The effects of plate configurations are investigated. These wind loading information are important for the design of billboards, the supporting frames and supporting column structures, eventually for the reduction of their vulnerability under wind loads.

2. Wind tunnel experiments

Wind tunnel experiments were conducted using No.3 Boundary Layer Wind Tunnel at the State Laboratory for Disaster Reduction of Civil Engineering in Tongji University, China. It is a closed-circuit type wind tunnel and is capable of generating wind speed up to 17.6 m/s. The boundary layer section of this wind tunnel is 15 m wide, 2 m high, and has a upstream fetch of 14 m for development of desired boundary layer wind flow. The wooden wedges in upstream of the boundary layer section and a combination of wooden roughness elements were used to simulate boundary layer flow. The mean wind speed profile was between those of open and suburban terrains as shown in Fig. 2(a) with a power law exponent of 0.2. The turbulent intensity profile is shown in Fig. 2(b), where the turbulence intensity decreases with height. The power spectrum of longitudinal turbulence at 100 cm above the ground (i.e., 20 m high in full-scale) is in good agreement with the von Kármán spectrum as shown in Fig. 3.The turbulence intensity and turbulence integral scale at the reference height of 100 cm are 7.6% and 42 cm, respectively.

Two typical billboard structures specified in Chinese code (CECS 148:2003),i.e., type G2-5×14 and G3-6×18, were selected for two-plate and three-plate configurations as shown in Fig. 4. The length scale ratio of the models is 1/20. The width (b) and height(c) of the sign faces as well as the overall height of the structures (h) and the angle between the plates (θ) are listed in Table1.

Table 1 Billboard prototype size list

Configuration	b (cm)	c (cm)	h (cm)	t (cm)	θ (°)
G2-5×14	70	25	89	6.2	4.5
G3-6×18	90	30	104	5	60

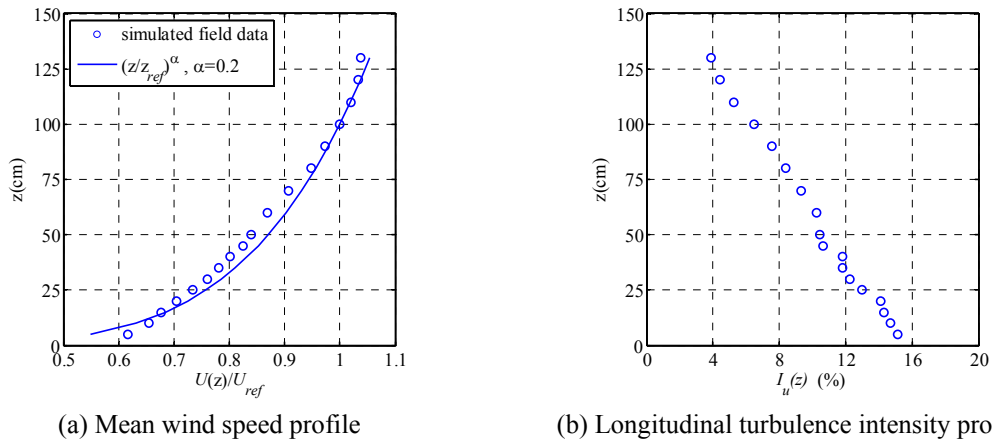(a) Mean wind speed profile   (b) Longitudinal turbulence intensity profile

Fig. 2 Mean wind speed and longitudinal turbulence intensity profiles of simulated boundary layer flow
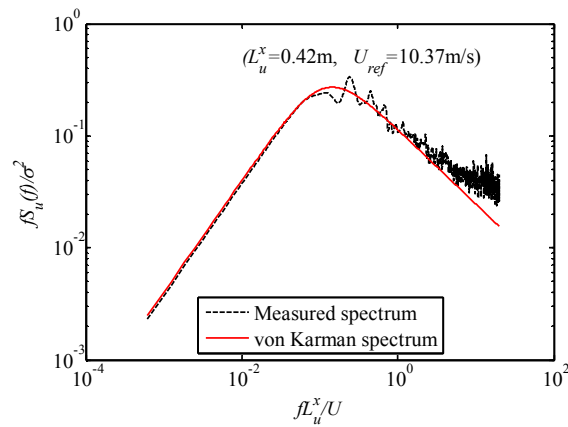
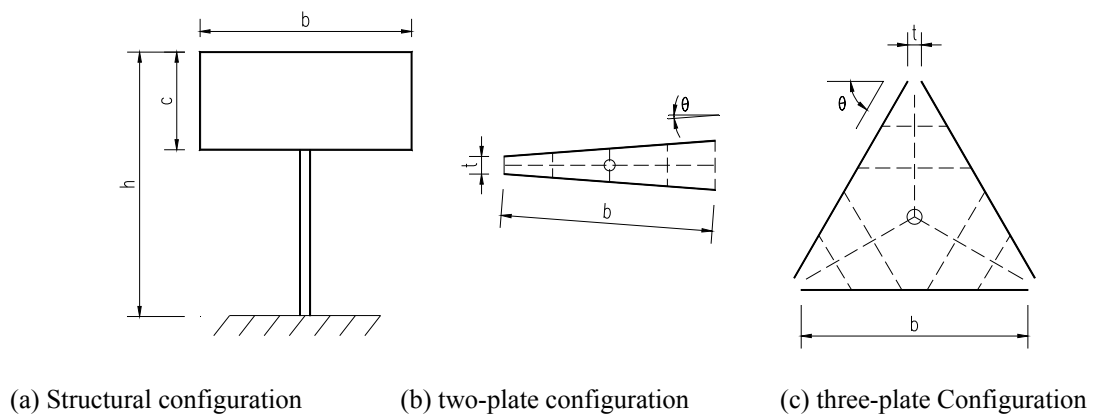Fig. 3 Power spectrum of longitudinal turbulence at 100 cm above the ground

(a) Structural configuration   (b) two-plate configuration   (c) three-plate Configuration

Fig. 4 Billboard models tested in wind tunnel

In order to measure the pressures on both windward and leeward sides of the billboard plate simultaneously, each billboard plate is constructed by a thin box of 2 cm thickness, made of light 3 mm thickness pine boards and ribs, permitting pressure tubes being inside the thin box. The pressure taps on both sides of the plate are placed at the same corresponding positions, thus the net pressure can be readily determined. The pressure tap distributions are shown in Figs. 5 and 6. In the case of two-plate model, each face consists of 90 pressure taps with a total of 90×4=360 taps used. For the three-plate model, there are 84 taps on each face with 84×6=504 taps in total.

To make model rigid and light, thin boxes are fixed with a supporting frame melted by aluminum bracing bars, then frame were connected with an aluminum column of 4 cm in diameter. Figs. 7 and 8 show the rectangular billboard models installed in the wind tunnel.

The wind direction of 0° is defined as wind perpendicular to the axis of symmetry of plates, and the wind direction increases clockwise as shown in Fig. 9. By using the turntable, the two-plate model was tested for 13 orientations ranging from -90° to +90° at 15° increments. The three-plate model was tested for 5 orientations ranging from -60° to +60° at 15° increments, and the symmetrical load characteristics can be assumed for the equilateral triangle three-plates billboard. The mean wind speed at the reference height (100 cm) is 10.37 m/s. The time scale factor is 4.47. At each wind direction, the wind pressures were recorded with a sampling frequency of 300 Hz and duration of 135 s, which correspond to a time step of 0.015 s and duration of 10 min in prototype.
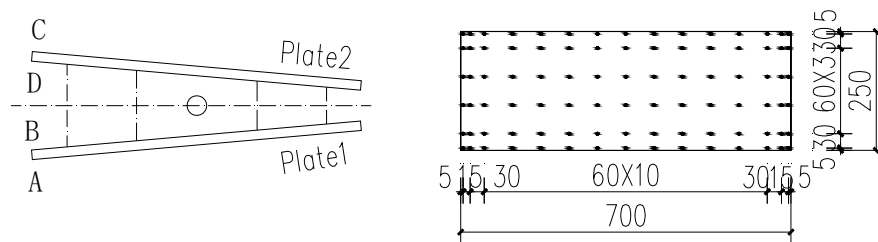

Fig. 5 Two-plate model and locations of pressure taps (unit of length: mm)
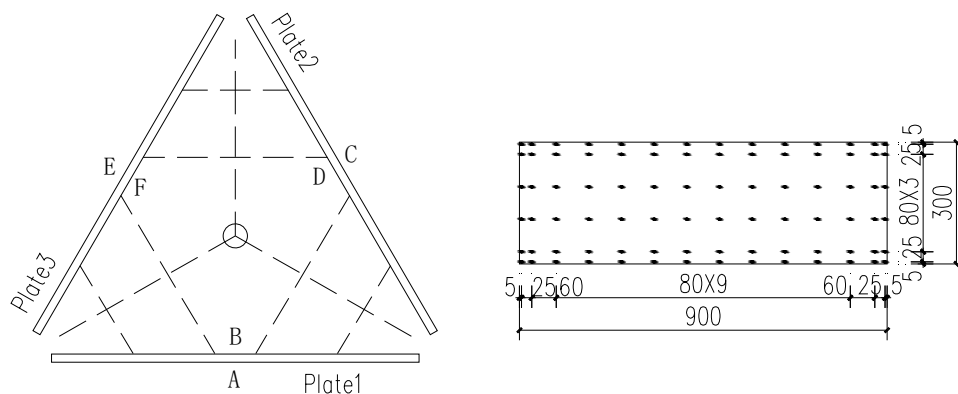

Fig. 6 Three-plate model and locations of pressure taps (unit of length: mm)
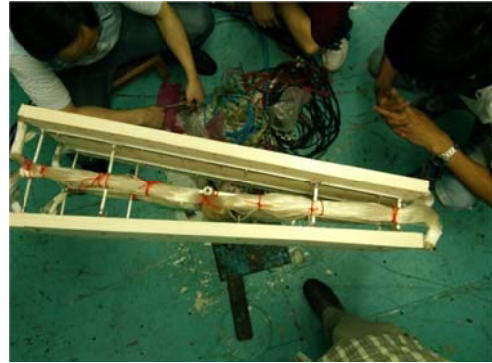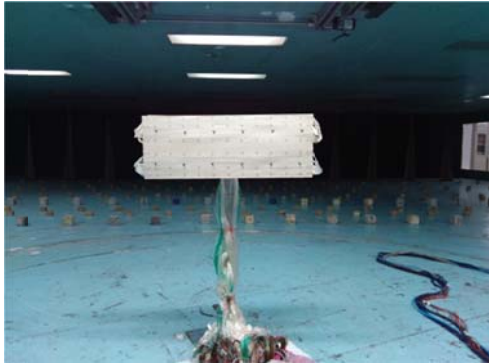
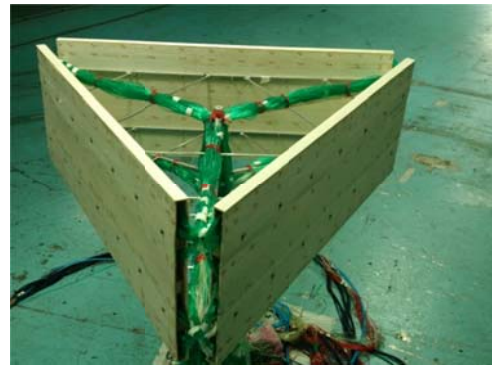Fig. 7 Two-plate model in the wind tunnel

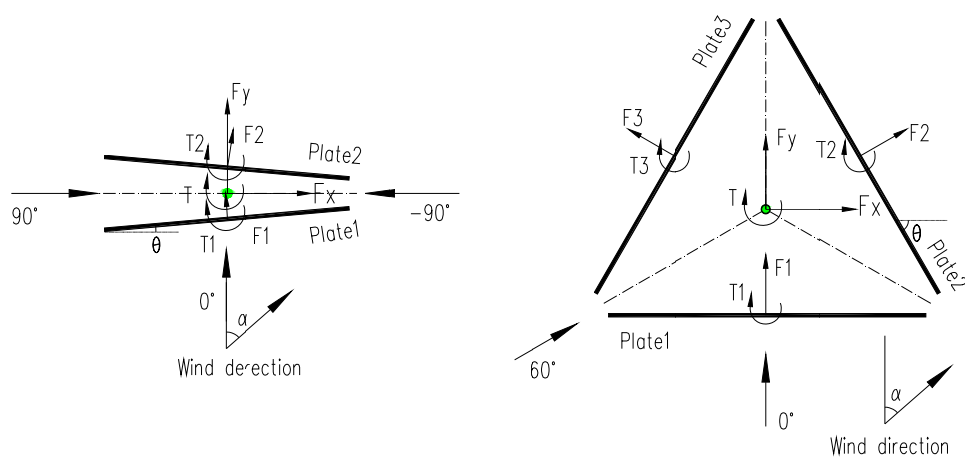Fig. 8 Three-plate model in the wind tunnel

Fig. 9 Wind direction and force coordination system

3. Results and discussions

3.1 Data interpretation

Based on the measurements of pressures, the net pressure at each tap location of the plates is calculated as the difference of pressures on both sides of the plates. The pressure coefficient is then defined as

$$C_{ij}(t) = p_{ij}(t) / (0.5\rho U_{ref}^2)$$

(1)

where $p_{ij}(t)$ is the net pressure at the *j*-th location of *i*-th plate; ρ is the air density; U_{ref} is the mean wind speed measured at the reference height, which is very close to the mean wind speed at the top of billboard model.

The integrated drag force and torque on each plate are then calculated as

$$F_i(t) = \sum_{j=1}^{n} p_{ij}(t) A_{ij}$$

$$T_i(t) = \sum_{j=1}^{n} p_{ij}(t) A_{ij} d_{ij}$$

(2)

where $F_i(t)$ and $T_i(t)$ are the drag force and torque of *i*-th plate; A_{ij} and d_{ij} are the tributary area and the horizontal distance (moment arm) from the center of sign face to the *j*-th pressure tap of *i*-th plate.

The drag force and torque coefficients are then defined as

$$C_{F_i}(t) = F_i(t) / (0.5\rho U_{ref}^2 bc)$$

$$C_{T_i}(t) = T_i(t) / (0.5\rho U_{ref}^2 b^2 c)$$

(3)

Where *b* and *c* are the width and height of the sign plate, respectively. The torque can also be represented as a horizontal eccentricity of the drag force from the plate center.

Based on the drag force and torque of each billboard, the overall drag force and torque can be computed as follows:

For the two-plate configuration

$$C_{F_X}(t) = \left(C_{F_2}(t) - C_{F_1}(t)\right) \sin\theta$$

$$C_{F_Y}(t) = \left(C_{F_1}(t) + C_{F_2}(t)\right) \cos\theta$$

$$C_T(t) = \sum_{i=1}^{2} C_{T_i}(t)$$

(4)

For the three-plate configuration

$$C_{F_X}(t) = \left(C_{F_2}(t) - C_{F_3}(t)\right) \sin\theta$$

$$C_{F_Y}(t) = C_{F_1}(t) + \left(C_{F_2}(t) + C_{F_3}(t)\right) \cos\theta$$

$$C_T(t) = \sum_{i=1}^{3} C_{T_i}(t)$$

(5)

3.2 Pressure distribution on the plate faces

Analysis of the pressure distribution is important for characterizing the wind load on billboard plates, and for examining skin damage of the plates. In the following, only the pressure distribution on the windward plate is discussed for the sake of brevity. The mean, standard deviation (STD) and extreme (peak), skewness and kurtosis of the net pressure coefficients on windward plate of two-plate billboard under wind directions of 0° and 45° are shown in Figs.10 and 11. The skewness and kurtosis are used to reveal the potential non-Gaussian distribution characteristics. The results for the three-plate configuration are shown in Figs.12 and 13.

It is observed that the characteristics of pressure coefficients on the windward plate in both two-plate and three-plate configurations are very similar, which are also similar to those of the single rectangular plate. When wind direction is normal to the windward plate, the pressures are symmetrically distributed across the plate. The pressure fluctuations follow almost Gaussian distribution with skewness close to zero and kurtosis close to three. Under the yaw wind direction, the pressures show oblique asymmetric distribution with gradient decreasing along windward direction. The wind fluctuations at the edges show clear non-Gaussian characteristics.

The local pressures, especially, the negative pressures, are responsible for the cladding damage of plates. Fig. 14 portraysthe largest positive and negative pressure coefficient distributions over all wind directions for both two-plate and three-plate configurations. The largest positive pressure on the two-plate configuration is observed near the up-right corner of the windward plate, i.e., plate 1, at wind direction of -60°.The peak pressure coefficient reaches 3.1, which is about 4 times of the mean pressure coefficient of 0.78.The largest negative pressure happens near the down-left corner of the leeward plate, i.e., plate 2, at wind direction of 60°. The peak pressure coefficient reaches -2.8, which is about 6 times of the mean pressure coefficient of 0.48.

(a) Mean

(b) STD
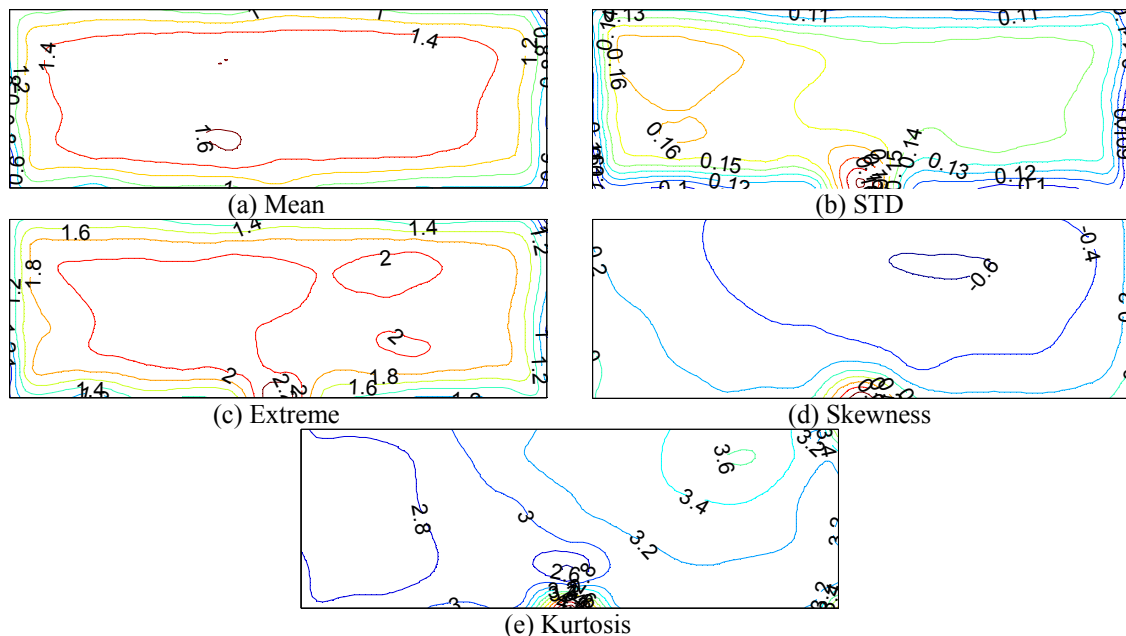
(c) Extreme

(d) Skewness

(e) Kurtosis

Fig. 10 Characteristics of pressure coefficients on the windward plate of two-plate model at wind directions of 0°
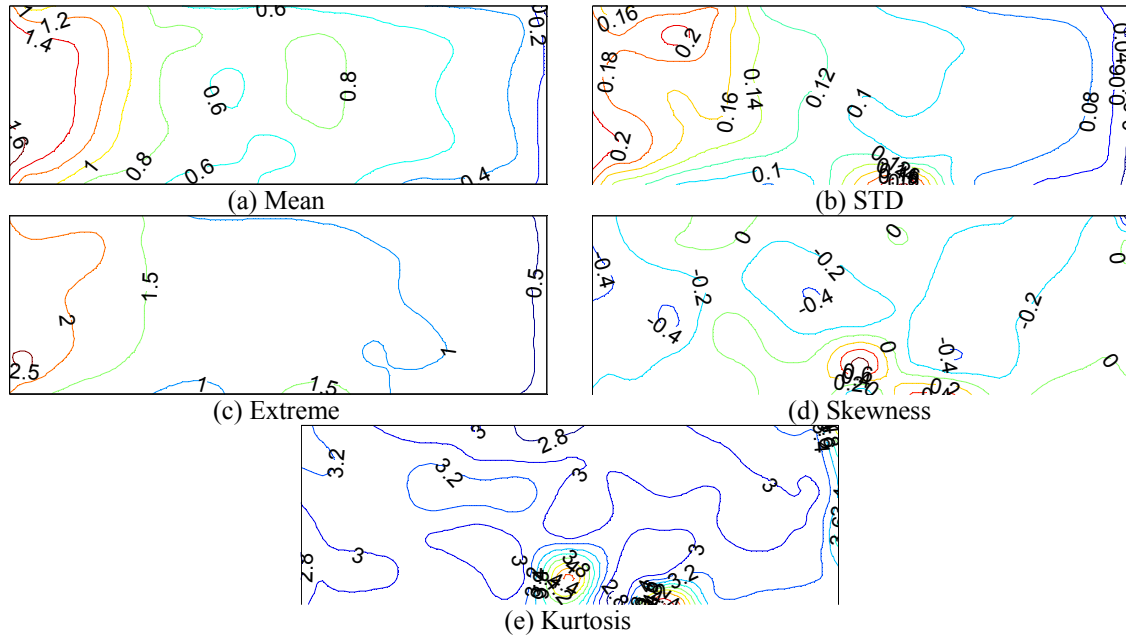
Fig. 11 Characteristics of pressure coefficients on the windward plate of two-plate model at wind directions of 45°
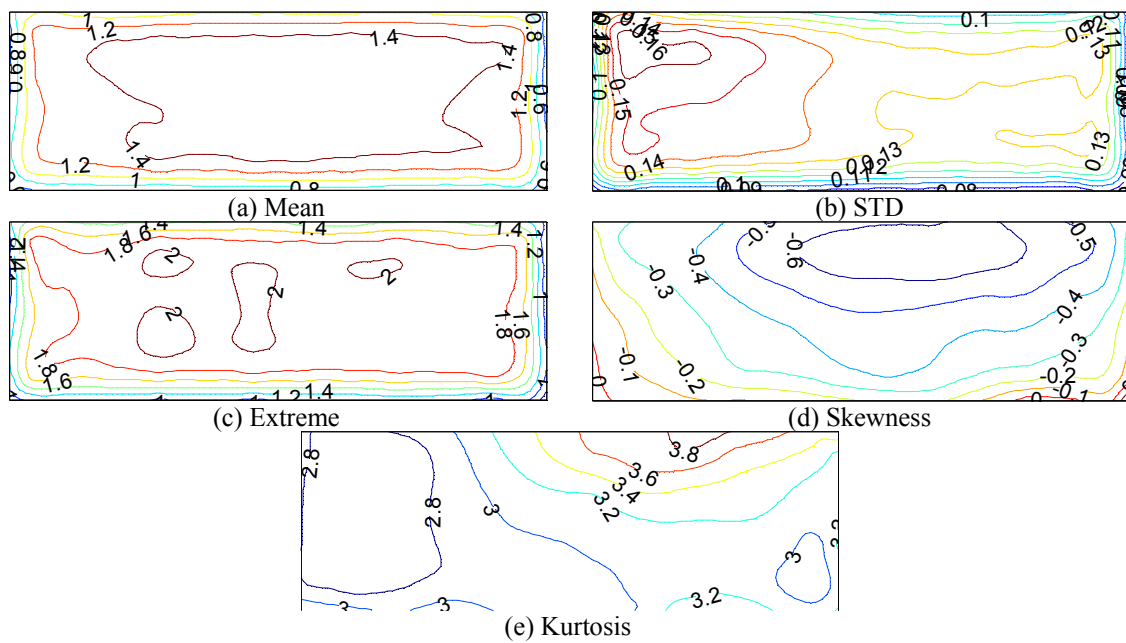

Fig. 12 Characteristics of pressure coefficients on the windward plate of three-plate model at wind directions of 0°

(a) Mean

(b) STD

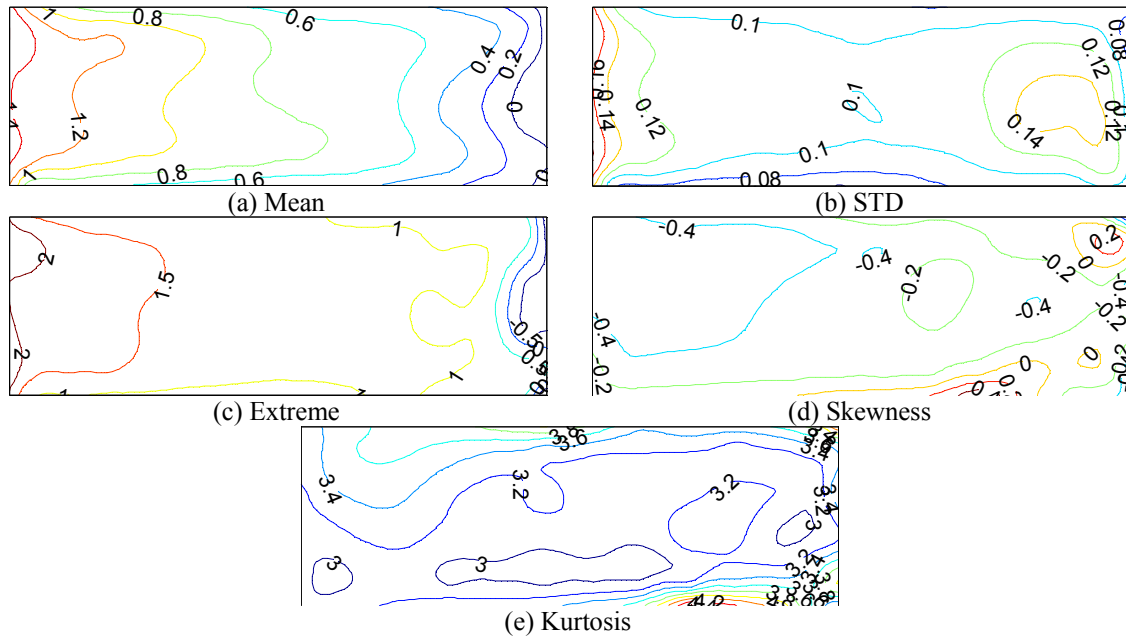(c) Extreme

(d) Skewness

(e) Kurtosis

Fig. 13 Characteristics of pressure coefficients on the windward plate of three-plate model at wind directions of 45°

As for the three-plates billboard as shown in Fig. 15, the largest positive pressures are along the side of the plate. The peak pressure coefficient reaches 3.4 observed on the windward plate, i.e., plate 1, at wind direction of 60°, which is about 7 times of the mean pressure coefficient of 0.474.The largest negative pressure happened near the width-wise side of the leeward plate 2. The peak pressure coefficient reaches -2.4 at wind direction of 45°, which is about 5 times of the mean force coefficient of 0.5.

(a) Positive

(b) Negative
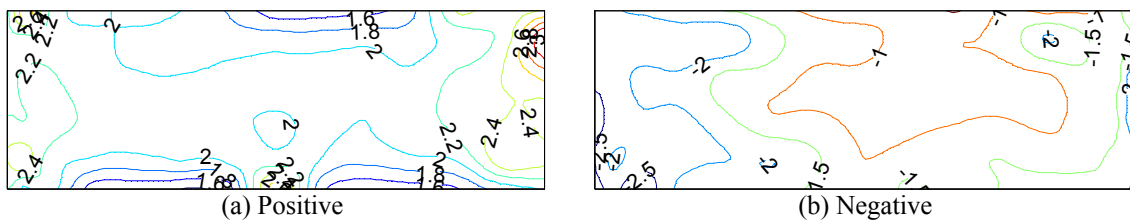
Fig. 14 Largest peak pressure coefficient distribution over all wind directions (two-plate configuration)
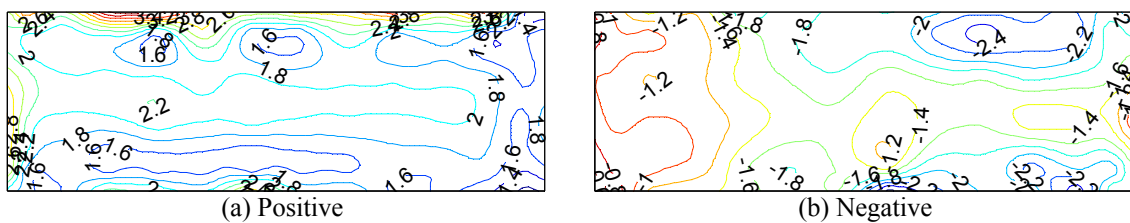

(a) Positive

(b) Negative

Fig. 15 Largest peak pressure coefficient distribution over all wind directions (three-plate configuration)

3.3 Wind loads on individual plates

3.3.1 Two-plate configuration

Design of billboard supporting structures requires quantification of wind loads on individual plates. Fig. 16 shows the mean, STD and maximum value of drag and torque coefficients of individual plates for two-plate billboard. The positive directions of the drag forces and torques are shown in Fig. 7. Fig. 17 displays their correlation coefficients. Table 2 summarizes the mean drag coefficients at a number of wind directions.

(a) Drag force coefficient, plate 1   (b) Torque coefficient, plate 1

(c) Drag force coefficient, plate 2   (d) Torque coefficient, plate 2
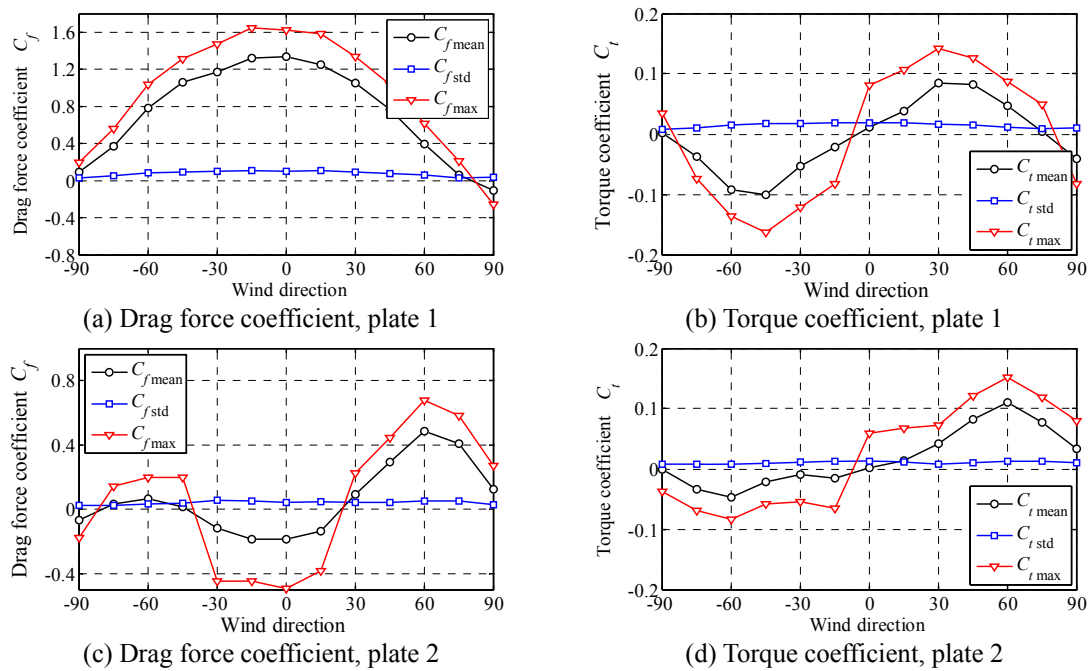
Fig. 16 Force coefficients of individual plate of two-plate configuration

(a) Plates 1 and 2   (b) Drag force and torque
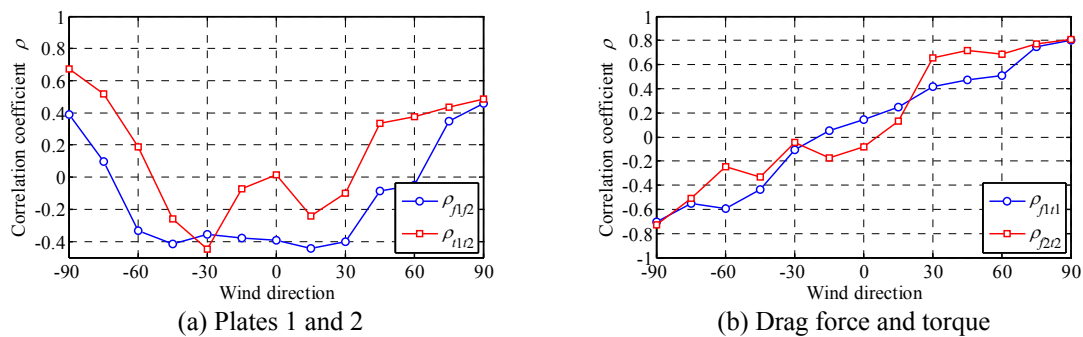
Fig. 17 Correlation coefficients between forces on individual plates of two-plate configuration

Table 2 Mean drag force coefficient of the plates of tow-plates billboard

Wind direction (°)	$C_{f\text{mean}}$				
	-60	-30	0	30	60
Windward plate	0.78	1.17	1.33	1.04	0.38
Leeward plate	0.06	-0.12	-0.19	0.09	0.48

The drag force on windward plate, i.e., plate 1, is a compressive force at all wind directions with a large mean component. The largest drag coefficient is observed around 0° with mean, STD and extreme force coefficients of 1.33, 0.1 and 1.62, which are slightly less than those of the single plate billboard (Letchford 2001, Warnitchai *et al*. 2009). The corresponding peak factor is 4.15, while the value is 3.89 calculated by the close-form formulation for the peak factor developed by Davenport (1964), $g = \sqrt{2\ln(v_0 T)} + 0.5772/\sqrt{2\ln(v_0 T)}$, where $v_0 = \sigma_{\dot{F}}/(2\pi\sigma_F) = 7.9$, σ_F and $\sigma_{\dot{F}}$ are the STD value of drag coefficient $C_{Fi}(t)$ and $\dot{C}_{Fi}(t)$, T=135 s is time duration in model scale. The distribution of the drag coefficient versus wind direction is close to the sine half-wave. The drag force on leeward plate, i.e., plate2, changes its direction with the change in wind direction. At the wind direction ranging from -30° to 30°, the mean dag force is in the opposite direction of that of windward plate 1. The mean and extreme drag force coefficients are -0.185 and -0.49 with a peak factor of 7.6 at wind direction of 0°. At other wind directions, the mean drag force on plate 2 is in the same direction as that of plate 1. The largest drag force coefficient is observed at wind direction of 60°with the mean, extreme and peak factor of 0.48, 0.67 and 3.7, respectively.

As expected, the torque coefficients of both plates vary with wind direction following approximate sine full-wave in magnitude with a direction change. The ratio of torque coefficient to the drag force coefficient at the same wind direction gives the eccentricity. For the simplicity of following discussion, the eccentricity of drag force at a given wind direction is defined as the ratio of the torque coefficient to the largest drag force coefficient over all wind directions. While this eccentricity definition does not represent the actual eccentricity of the drag force, it is convenient to represent the magnitude of the torque coefficient as a function of wind direction. The largest extreme torque coefficient at plate 1, i.e., windward plate, is observed as -0.16, in term of an eccentricity of 0.1b, at wind direction of 45°, which corresponds to the extreme drag coefficient of 1.31, i.e., 80% of the largest drag coefficient over all directions. It is evident that in the case of plate 1, the large value of drag coefficient, which is observed at wind directions close to the direction normal to the plate, corresponds to a low level of torque coefficient. The largest eccentricity is found at wind directions of ± 45° in which the drag force coefficient is relatively low. As for the plate 2, the largest torque coefficient is observed as 0.15, in term of the eccentricity of 0.22b at wind direction of 60°. At this wind direction, the largest drag coefficient of 0.67 over all directions is observed.

Regarding the correlation coefficients of the force components on individual plates, it is evident that around the wind direction of0°where the largest drag force coefficient on plate 1 is observed, the correlation between the drag force and torque of each plate is very low thus can be considered to be statistically independent. The correlation coefficient of both drag forces of the two plates are

-0.4. As expected, the correlation coefficients alter with wind direction.

The skewness and kurtosis of the force and torque coefficients at different wind directions are also calculated. In case of windward plate, it is observed that the skewness and kurtosis of the drag force coefficient are -0.43 and 3.13 at wind direction of 0°. The maximum skewness and kurtosis of these are -0.59 and 3.5, both at wind direction of 15°. The maximum skewness and kurtosis of the leeward plate are -0.70 and 4.3 at wind direction of 0°. As for the torque coefficient of the windward plate, the maximum skewness and kurtosis are -0.48 and 3.18, both at wind direction of 60°. These of the leeward plate are -0.14 and 3.2 at wind direction of around 60°. It is evident that while the drag force on the leeward plate show some non-Gaussian properties at wind direction of around 0°, other integrated drag and torques are primarily Gaussian processes.

3.3.2 Three-plate configuration

The results of drag forces and torques on individual plates of three-plate configuration are portrayed in Figs.18 and 19. The mean drag force coefficients at a number of wind directions are summarized in Table 3. The characteristics of drag force and torque on windward plate are almost identical to those of two-plate configuration. The largest drag force coefficient is observed as at wind direction of 0° with mean and extreme values of 1.24 and 1.57, respectively, which are less than those of the windward plate of two-plate billboard mentioned previously, as well as those of single plate billboard (Letchford 2001, Warnitchai *et al.* 2009). The corresponding peak factor is 3.67, while the value is 4.03 calculated by the close-form formulation for the peak factor developed by Davenport (1964). The corresponding extreme torque coefficient at the same wind direction is 0.08, i.e., 0.05b in terms of eccentricity. At wind direction of 60°, the force characteristics of plates 1 and 3 are very close due to the geometric symmetry, and the drag force on plate 2 reaches its maximum with a mean and extreme drag coefficients of 0.59 and 0.8 in the along-wind direction. The largest extreme torque coefficient is observed on the windward plate at wind direction of 60°, which is 0.15, i.e., 0.1b in terms of eccentricity.

The correlations among the drag forces of three plates in three-plate configuration are weak compared with the two-plate configuration model. The correlation between drag force and torque on each individual plate is also weak, while the correlation coefficient between drag force and torque on plates 2 is higher.

The maximum skewness and kurtosis of the drag force coefficient of plate 1 are -0.53 and 3.6, both at wind direction of 30°. While these of plate 2 are 0.23 and 3.38 at wind direction of 30°, and those of plate3 are 0.30 and 3.35 at wind direction of around 60°. The skewness and kurtosis of the torques at individual plates are also calculated. The results show that the integrated drags and torques on individual plates can be considered as Gaussian processes.

Table 3 Mean drag force coefficient of the plates of three-plates billboard

Wind direction (°)	C_{fmean}				
	0	15	30	45	60
Windward plate 1	1.24	1.20	1.01	0.74	0.474
Leeward plate 2	0	0	0.20	0.50	0.6
Leeward plate 3	0	0	-0.11	-0.22	-0.47

(a) Drag force coefficient, plate 1

(b) Torque coefficient, plate1

(c) Drag force coefficient, plate 2

(d) Torque coefficient, plate2

(e) Drag force coefficient, plate3

(f) Torque force coefficient, plate3
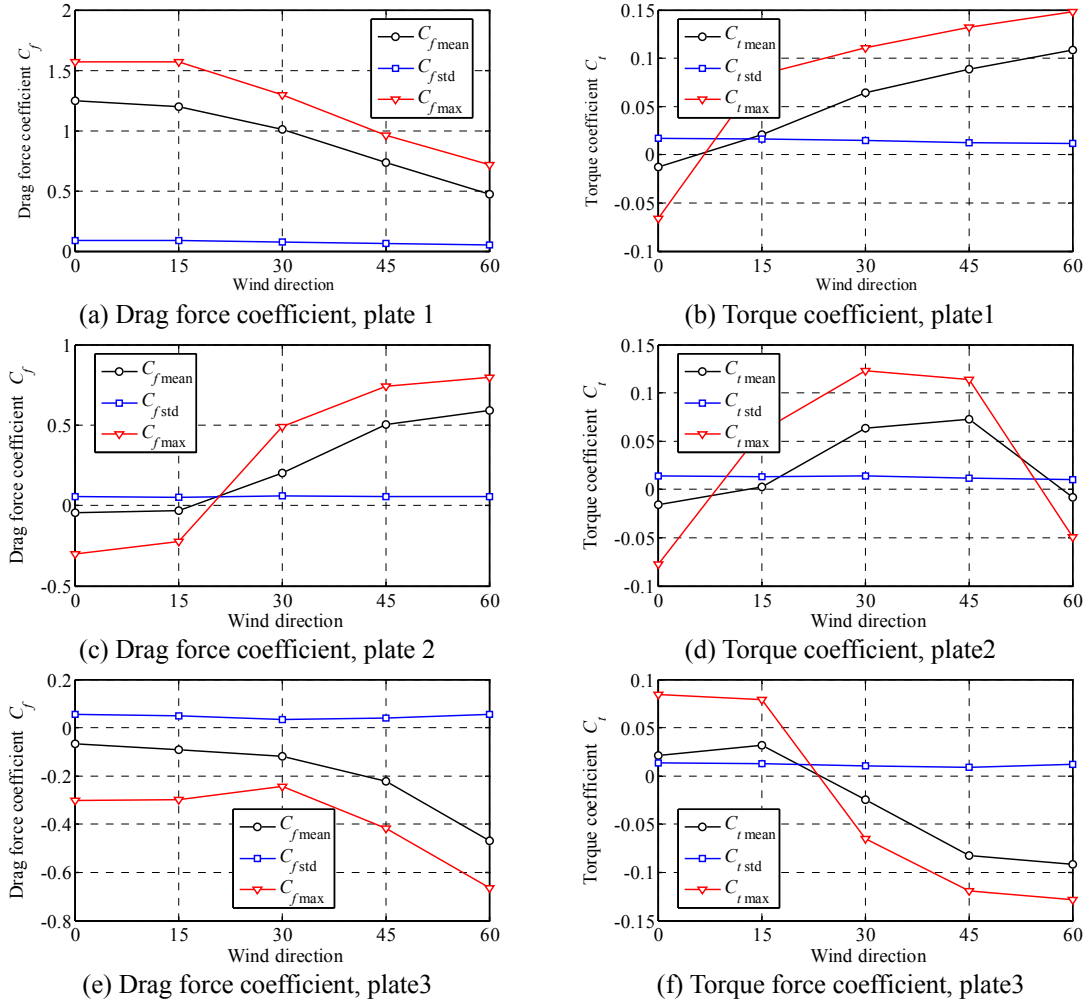
Fig. 18 Force and torque coefficients of individual plate of three-plate configuration

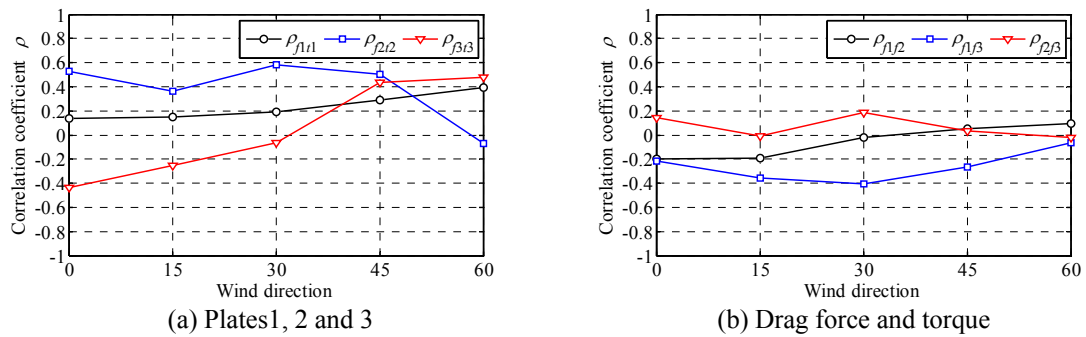(a) Plates1, 2 and 3

(b) Drag force and torque

Fig. 19 Correlation coefficient between forces and plates of three-plate configuration

3.4 Wind load on overall board

3.4.1 Two-plate configuration

The mean, STD and maximum of overall force coefficients in two orthogonal directions and torque coefficient for the two-plate configuration are given in Figs. 20(a)-20(c). The correlation coefficients are shown in Fig. 20(d). It is observed that the overall drag coefficient in the alongwind direction is not sensitive to wind direction in the range of -45° to 45°. The values of alongwind drag coefficient is close to the results of field measurement and win tunnel experiment reported in Zuo *et al*. (2014) and Smith *et al*. (2014), but is slightly less than those of the experiments reported in Letchford *et al*. (2001) and Warnitchai *et al*. (2009). The largest mean and maximum values reach 1.15 and 1.42 at wind direction of 0°, respectively. The crosswind force coefficient is relatively low with the largest mean and extreme values of -0.11 and -0.15 at wind direction of 0°. The largest torque coefficient happens within wind direction of -60° to -45°, and 45° to 60°, with mean and extreme values of 0.16 and 0.23, respectively. The largest torque corresponds to an eccentricity of 0.16b when normalized with respect to the largest drag at wind direction of 0°. This result is consistent with those reported in literature (Letchford 2001, Warnitchai *et al*. 2009, Zuo *et al*. 2014), and is lower than value of 0.2b specified in design codes and standards (ASCE/SEI 7-10; AS/NZS 1170.0:2011). The overestimate of the torque is particularly true by further considering the fact that the largest drag and torque do not take place at same wind direction. The STD coefficients of alongwind and crosswind forces are not sensitive to wind direction, which are among 0.06-0.09. The correlation coefficient is given in Fig. 20(d), which is consistent to the field measurement results (Smith et al., 2014)

The supporting column is typically of a tubular cross section. The influence of the crosswind force can be investigated by its contribution to the resultant force coefficient

$$C_F = \sqrt{C_{F_x}{}^2 + C_{F_y}{}^2} \tag{6}$$

For the simplicity and conservative of computation, the maximum values of alongwind and crosswind forces are combined. The resultant force coefficients at different wind directions are displayed in Fig. 21(a). The comparison of Figs. 20(a) and 21(a) demonstrates that the contribution of crosswind force is negligible.

The contribution of torque is further investigated by calculating the resulting quasi-static shear stress as compared with the quasi-static bending normal stress caused by the alongwind force at the base of supporting column. The normal and shear stresses are estimated as

$$\sigma_{max} = F_y H(D/2)/I$$
$$\tau_{max} = T(D/2)/J \tag{7}$$

and their ratio is

$$\beta = \tau_{max}/\sigma_{max} = 2T/(F_y H) \tag{8}$$

where I and J are moment of inertial and polar moment of inertial of the section, and $J=2I$ for a tubular cross section; D is outer diameter of the tubular cross section; and H is the height of the supporting column, say, 15.5 m. The stress ratios at different wind directions are shown in Fig. 21(b). The shear stress caused by the torque is quite low at the base of the supporting column. The shear stress will be relatively large for cross sections at upper heights of the column.
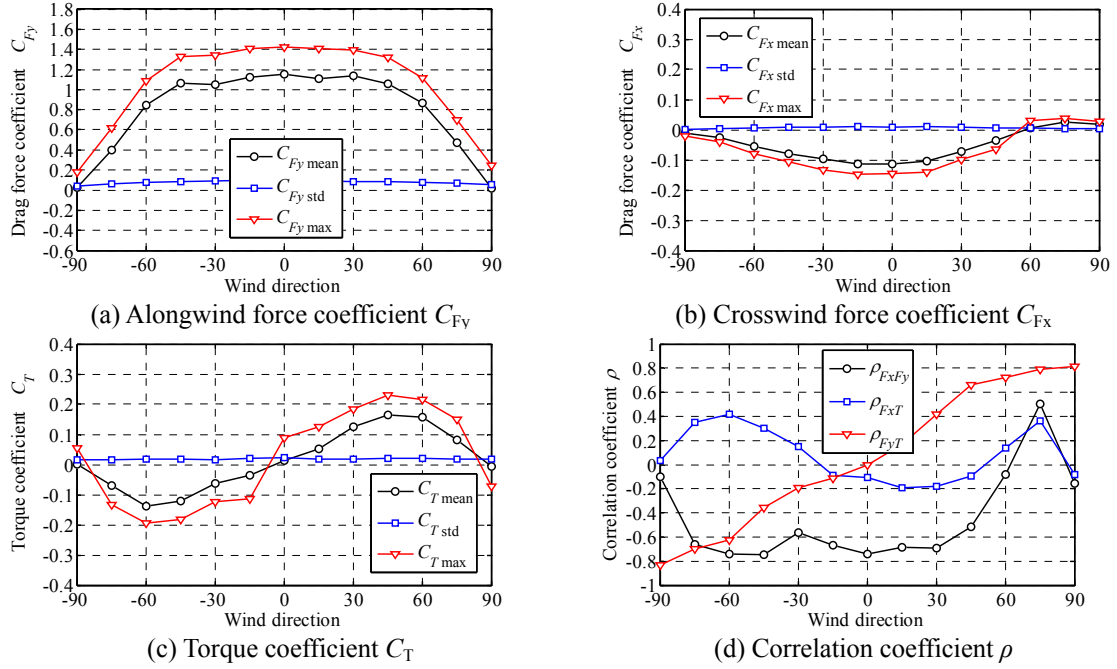
(a) Alongwind force coefficient C_{Fy}

(b) Crosswind force coefficient C_{Fx}

(c) Torque coefficient C_T

(d) Correlation coefficient ρ

Fig. 20 Overall forces and torque coefficients and their correlation of two-plate configuration versus wind direction

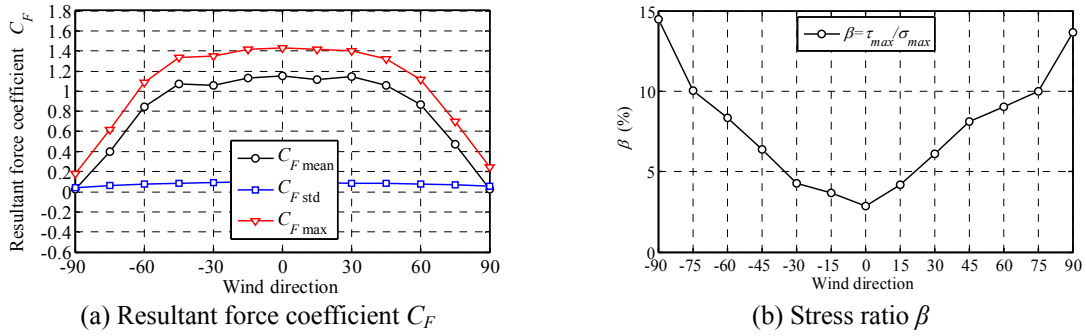(a) Resultant force coefficient C_F

(b) Stress ratio β

Fig. 21 Overall resultant drag force coefficient CF and the stress ratio β versus wind direction

3.4.2 Three-plate configuration

The mean, STD and maximum of overall forces and torque coefficients in the case of three-plate configuration are given in Figs. 22(a)-22(c). The correlation coefficients are shown in Fig. 22(d). It is observed that the overall drag coefficient in the alongwind direction decreases while the force in the crosswind direction increases with wind direction yawing from 0° to 60°. The mean and maximum values of alongwind drag coefficient reach 1.18 and1.51 at wind direction of 0°, respectively. The crosswind force coefficient is little lower with the largest mean and extreme values of 0.92 and 1.14 at wind direction of 60°. The STD coefficients of alongwind and crosswind forces are not sensitive to wind direction, which are among 0.06-0.09. The largest overall torque coefficient happens at wind direction of 30°, with mean and extreme values of 0.1

and 0.17, respectively. These are 0.10b in terms of eccentricity when normalized with respect to the largest alongwind force at wind direction of 0°.

As discussed previously, the influence of the crosswind force can be investigated by its contribution to the resultant force coefficient C_F as shown in Eq. (6). As shown in Fig. 22(a) and compared with Fig. 23(a), the contribution of crosswind force is noticeable particularly at larger yaw angle. It makes the resultant force coefficient less sensitive to yaw angle. The mean and extreme value of resultant drag force coefficient C_F reach 1.2and 1.6, respectively, which are close to that of two-plate billboard. As shown in Fig. 23 (b), the shear stress caused by the torque is quite low at the base of the supporting column.
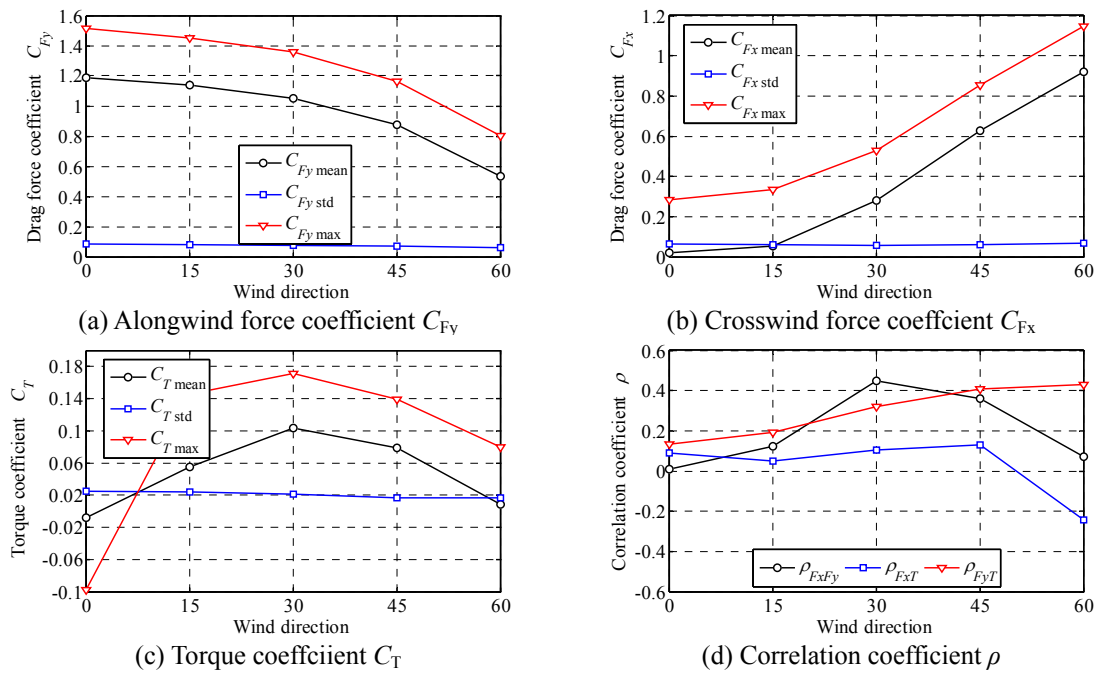

(a) Alongwind force coefficient C_{Fy}

(b) Crosswind force coeffcient C_{Fx}

(c) Torque coeffciient C_T

(d) Correlation coefficient ρ

Fig. 22 Overall force and torque coefficients and their correlation of three-plate configuration versus wind direction
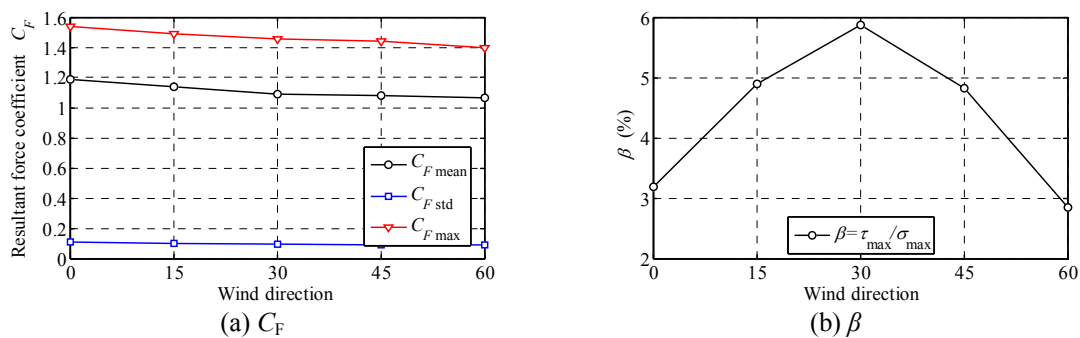

(a) C_F

(b) β

Fig. 23 Overall resultant drag force coefficient and the stress ratio of three-plate configuration versus wind direction

4. Conclusions

This paper presented the outcome of a comprehensive wind tunnel study conducted to investigate the wind loading of large billboard structures. The following conclusions can be revealed:

The characteristics of positive pressure on the windward plate in both two-plate and three-plate configurations are very similar with those of the single rectangular plate. For the intensive local negative pressures which are responsible to the cladding damage, the largest local negative net pressure coefficient at wind direction of around 60° would reach -2.8 and -2.4 for the two configurations at the edges of board with strong non-Gaussian characteristics. Pressures on the leeward plate of two-plate configuration show the positive under normal wind direction.

The results of integrated drag force on individual plate in the two configuration reveal significant influence of the position and wind direction. The largest compressive coefficient on windward plate is observed at normal wind direction, and the value is a slightly less than that of the single plate, while the largest suction force coefficient on leeward plate is observed at wind direction of 60°. The largest eccentricity of these two configuration are both at 60° wind direction, which are lower than the value specified in current codes and standards. The correlation of the force components on individual plates are quite low.

The overall alongwind and crosswind forces reveals significant influence of the configurations and wind directions. The largest alongwind drag force coefficient, i.e., at normal wind direction, is much less than that of the single plate. In the case of two-plate configuration, the contribution of crosswind force to the total resultant force is negligible. For three-plate configuration, the contribution of crosswind force is noticeably large which makes the total resultant force less sensitive to wind directions from -45° to 45°. The overall torques are lower than the values specified in current codes and standards. The contribution of torque to the overall stress at the base of column is insignificant.

The above findings on the local net pressure distributing, force and torque coefficient on the plates of the two configures of large billboard help in the development of more rational wind load standard for large billboard structures in the future.

Acknowledgements

References

An, S. (2009), *Wind disaster vulnerability study of single-column billboard structure*, Ph.D. Dissertation, Harbin Institute of Technology, Harbin. (In Chinese)
AS/NZS 1170.0:2011 (2011), Structural Design Actions Part 2: Wind actions – Standards New Zealand, Wellington., New Zealand.
ASCE/SEI 7-102010 (2010), *Minimum design loads for buildings and other structures*, American Society of Civil Engineers, Reston, VA, USA
CECS 148:2003 (2003), Technical specification for steel structures of outdoor advertisement facility.

Beijing, China.

Davenport A.G. (1964), "Note on the distribution of the largest value of a random function with application to gust loading", *Proc. Instn. Civ. Engng.*, **28**, 187-196.

GB50009-2012 (2012), Load Code for the Design of Building Structures, Beijing, China.

Gu, M., Lu, W., Han, Z. and Zhou, X. (2015), "Characteristics of wind pressure distribution on large single column supported billboards", *Tongji Daxue Xue bao/Journal of Tongji University*, **43**(3), 337-344. (In Chinese)

Letchford, C.W. (2001), "Wind loads on rectangular signboards and hoardings", *J. Wind Eng. Ind. Aerod.*, **89**, 135-151.

Letchford, C.W. and Holmes, J.D. (1994), "Wind loads on free-standing walls in turbulent boundary layers", *J. Wind Eng. Ind. Aerod.*, **51**, 1-27.

Letchford, C.W. and Robertson, A.P. (1999), "Mean wind loading at the leading ends of free standing walls", *J. Wind Eng. Ind. Aerod.*, **79**, 123-134.

Martinez-Vazquez, P., Baker, C.J., Sterling, M., Quinn, A. and Richards, P.J. (2010), "Aerodynamic forces on fixed and rotating plate", *Wind Struct.*, **13**(2), 127-144.

Meyer, D., Chowdhury, A.G. and Irwin, P. (2015), "Investigation of wind-induced dynamic and aeroelastic effects on variable message signs", *Wind Struct.*, **20**(6), 793-810.

Smith, D.A., Zuo, D. and Mehta, K.C. (2014), "Characteristics of wind induced net drag force and torque on a rectangular sign measured in the field", *J. Wind Eng. Ind. Aerod.*, **130**, 62-67.

Song, F. and Ou, J. (2009), "Study on the dynamic causes of damage of large billboard by typhoon", *Proceedings of the 14th National Conference of Structural wind engineering*, Beijing, August. (In Chinese)

Tamura Y. and Cao, S. (2009), "Climate change and wind-related disaster risk reduction", *Proceedings of the APCWE-VII*, Taipei, November.

Warnitchai, P., Sinthuwong, S. and Poemsantitham, K. (2009), "Wind tunnel model tests of large billboards", *Adv. Struct. Eng.*, **12**(1), 103-114.

Zuo, D., Letchford, C.W. and Wayne, S. (2011), "Wind tunnel study of wind loading on rectangular louvered panels", *Wind Struct.*, **14**(5), 449-463

Zuo, D., Smith, D.A. and Mehta, K.C. (2014), "Experimental study of wind loading of rectangular sign structures", *J. Wind Eng. Ind. Aerod.*, **130**, 62-74.

AD